ChemComm

Multi-layer Core/Shell Microgels with Internal Complexity and their Nanocomposites

Journal:	*ChemComm*
Manuscript ID	CC-COM-11-2023-005579.R2
Article Type:	Communication

COMMUNICATION

Multi-layer Core/Shell Microgels with Internal Complexity and their Nanocomposites

Received 00th January 20xx,
Accepted 00th January 20xx

DOI: 10.1039/x0xx00000x

Haruka Minato,[‡a] Satoki Ushida,[‡a] Kentaro Yokouchi,[a] and Daisuke Suzuki*[ab]

In this study, we show that core/shell (CS) microgels with multiple layers can be created *via* a one-pot precipitation polymerization, in which monomers are added to the reaction flask multiple times once most of the previous monomer has been consumed. The complex internal structures of the microgels were examined using a combination of scattering and microscopy techniques.

Hydrogel microparticles (microgels or nanogels) are colloids with a water content of >90%. The greater softness of microgels compared to conventional rigid colloids based on e.g., polystyrene or silica leads to fascinating properties and functions, including the uptake/release of functional molecules,[1] deformation at fluid interfaces,[2] and stimuli-responsiveness.[3] Like conventional rigid colloids, microgels also have great potential as building blocks for the assembly of bulk materials.[4] In order to improve the properties and functions of microgels, precise control of their nanostructures is desired.

The construction of core/shell (CS) structures is a useful strategy to create new functional materials.[5] To date, various types of CS microgels, including solid-core/hydrogel-shell microgels,[6] CS microgels composed entirely of hydrogels,[7] double-shell CS microgels,[8] hollow microgels,[8cd,9] yolk–shell-type microgels,[8b,10] and CS microgels with shape anisotropy[11] have been developed. These CS microgels are typically prepared via aqueous free radical seeded precipitation polymerization, whereby the monomers for shell synthesis are water-soluble, while the growing polymers become water-insoluble during polymerization and the resultant globular polymers attach to the pre-existing cores.[1a,7,12] The creation of CS structures allows the realization of complex properties and functions that cannot be achieved by their parent cores.

However, compared to classical solid-core/soft-hydrogel-shell microgels, the structure of CS microgels composed entirely of hydrogels is complex, as the core microgel structure can change during the shell-formation process,[13] which hinders the evaluation of the precise structural design of CS microgels. For instance, unlike for CS particles with multiple layers composed entirely of non-hydrogels,[14] the inner structure of microgels is difficult to investigate due to undesired compression from the outer shell during sample preparation.[13] Therefore, various techniques have been developed to determine the structure of CS microgels.[15-17] For instance, small-angle neutron scattering data, in conjunction with a developed form-factor model described by a two-box profile based on the hydrogel core and shell, can be used to supply quantitative information on the internal structure of a CS microgel.[15] In addition, fluorescence resonance energy transfer analysis of donor-/acceptor-labelled CS microgels allows for the precise calculation of core size and shell thickness.[16] However, to the best of our knowledge, there are no reports on the synthesis and characterization of CS microgels with more than two shell layers based on these methods, which is presumably due to the structural complexity of multi-layer CS microgels.

In the present study, we accomplished the synthesis of CS microgels with multiple layers via a one-pot precipitation polymerization, in which monomer solutions for the formation of shell layers were added to the flask during the precipitation polymerization at multiple time points (Fig. 1). To evaluate the spatial distribution inside the CS microgels, we used scattering measurements and a labelling technique in which rigid nanoparticles (e.g., polystyrene) are selectively introduced inside the microgels, which has previously been investigated by our groups.[3c]

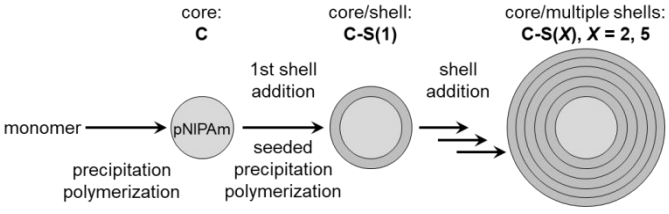

Fig. 1 Schematic illustration of the one-pot synthesis of core/shell microgels with multiple layers *via* precipitation polymerization and seeded precipitation polymerization.

In this study, poly(*N*-isopropyl acrylamide) (pNIPAm)-based microgels were selected as model multi-layer microgels given that their characteristics have been extensively

[a] *Graduate School of Textile Science & Technology, Shinshu University, 3-15-1 Tokida, Ueda, Nagano 386-8567, Japan*
[b] *Research Initiative for Supra-Materials, Interdisciplinary Cluster for Cutting Edge Research, Shinshu University, 3-15-1 Tokida, Ueda, Nagano 386-8567, Japan*
‡ *These authors contributed equally. E-mail: d_suzuki@shinshu-u.ac.jp (D.S.)*
Electronic Supplementary Information (ESI) available: [details of any supplementary information available should be included here]. See DOI: 10.1039/x0xx00000x

investigated.[1a,3ad] First, core microgels composed of pNIPAm chemically cross-linked with *N,N'*-methylenebis(acrylamide) (BIS) were synthesized *via* conventional precipitation polymerization.[3ac] Microgels prepared by aqueous precipitation polymerization are known to show concentric growth and uniform size in spherical. [3c,12] During the polymerization, phase separation of the thermoresponsive polymers occurs, and the dehydrated and globular polymer chains self-assemble into spherical particles.[3c,12]

In our previous study, we found that hydrophobic monomers such as styrene avoid polyelectrolyte regions when they are transformed into hydrophobic nanoparticles inside pNIPAm-based microgels.[17] The hydrophobic nanoparticles in the resulting composites can be visualized using transmission electron microscopy (TEM) of ultrathin cross-sections of the resulting nanocomposite microgels, which provides information on the structure of the gels.[17] Therefore, to clarify the formation of CS structures with multiple layers as shown in Fig. 1, the shell layers were constructed by chemically (BIS)-crosslinking monomers with charged (carboxyl) groups, i.e., methacrylic acid (MAc) or fumaric acid (FAc), and NIPAm to form the copolymer shells. pNIPAm-*co*-MAc was chosen for the inner shells of the multi-shell microgels, given that MAc-rich polymer chains are formed in the early stage of the free radical precipitation polymerization due to the reactivity ratio (r_{NIPAm} = 0.2; r_{MAc} = 2.8),[18] and we thus assumed that the charged groups (i.e., carboxyl groups) of MAc would be localized on the inner surface of the shell layers, even though the copolymer chains were assembled on pre-existing cores. Thus, it was expected that the polystyrene nanoparticles would avoid the MAc-rich region in the shells. The outermost shell consisted of pNIPAm-*co*-FAc, because, unlike MAc, FAc is consumed in the final stage of radical copolymerization (r_{NIPAm} = 7.0; r_{FAc} = 0.09),[18] and thus the carboxyl groups of FAc can be expected to be localized at the outer surface of the shell layers, which would be important for stabilization during the seeded emulsion polymerization of styrene to form the nanocomposites.[19] It is worth noting here that no studies of the spatial distribution of such charged copolymers in the shells of CS microgels have been reported to date.

To obtain microgels with different numbers of shell layers, aqueous solutions of NIPAm and MAc (or FAc) with the chemical crosslinker BIS were added to the reaction solution after the previous batch of monomers had mostly been consumed (i.e., *ca.* 1 h after the initiation or addition of comonomer solutions). Here, CS microgels are denoted as C-S(*X*), where C and S refer to the core and shell layers, respectively, and *X* represents the number of shell additions.

First, CS microgels with two shell layers, C-S(2), were synthesized as shown in Table S1 in the ESI. The size uniformity and size increase of the microgels were investigated using field emission scanning electron microscopy (FE-SEM) (Fig. 2(a)). Fig. 2(a) demonstrates the successful preparation of the C-S(2) microgels, as the diameter (*D*) of the microgels increased stepwise upon adding shell monomers (i.e., C-S(2): *D* = 265 nm (core) → 447 nm (1st shell addition) → 484 nm (2nd shell addition)), indicating that the pNIPAm-based polymers are effectively adsorbed onto the pre-existing cores, and that the resultant microgels are uniform in size (CV < 10%) without secondary particle formation during shell synthesis. Unlike in our previous report on the synthesis of microgels with multiple layers, in which the hydrogel shell was added onto pre-existing microgels, and the core microgels were purified before each shell addition,[17] the method shown in Fig. 1 does not require successive purifications before each shell addition, and is thus less time-consuming.

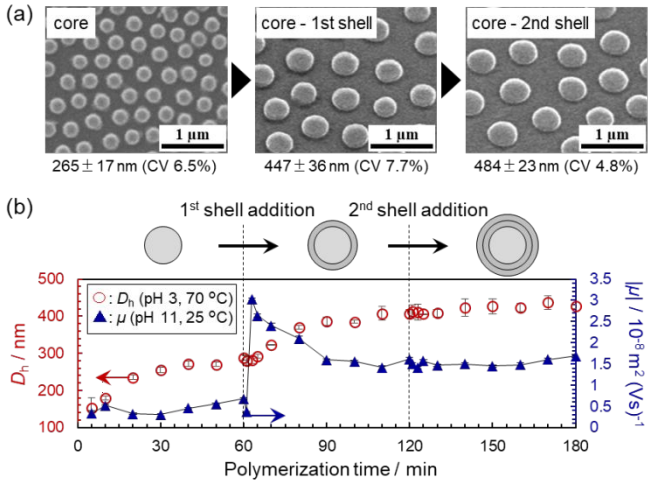

Fig. 2 (a) Representative SEM and FE-SEM images of the C-S(2) microgels (*N* = 200). (b) Hydrodynamic diameter (D_h) and absolute value of the electrophoretic mobility ($|\mu|$) for C-S(2) microgels under different temperature/pH conditions at different polymerization times, as determined using dynamic light scattering (DLS) and electrophoretic light scattering (ELS), respectively. It should be noted here that all microgels studied exhibited negative μ values due to the presence of residual initiator and MAc or FAc.

The evolution of the hydrodynamic diameter (D_h) of the CS microgels was calculated using dynamic-light-scattering (DLS) data during polymerization. It should be noted here that the microgels were characterized in a deswollen state (i.e., pH = 3, 70 °C)[20] in order to avoid any microgel-swelling effects (i.e., shell-restricted core compression[13] and/or osmotic pressure[21] originating from the carboxyl groups). For the C-S(2) microgels, the D_h of the core microgels increased gradually and reached a constant value after 40 min (40 min: 272 nm; 60 min: 287 nm) (Fig. 2(b)). After the addition of shell monomer at 60 min, the D_h increased further, plateauing within 30 min (Fig. 2(b)). The second addition of shell monomer to form the outermost layer at 120 min led to a further increase in D_h (Fig. 2(b)). It should also be noted here that the D_h showed a linear rather than a stepwise increase when shell monomers were added every 20 min (Fig. S1, ESI).

The electrophoretic mobility (μ) of the C-S(2) microgels was evaluated using electrophoretic light scattering (ELS) to clarify their surface properties, as μ can be an indicator of the surface charge density of microgels.[22] For that purpose, microgels with deprotonated carboxyl groups (pH = 11) were examined in a swollen state at 25 °C. The absolute electrophoretic-mobility values ($|\mu|$) increased significantly after 63 min, i.e., almost immediately after adding the first batch of shell monomers (NIPAm, MAc, and BIS), and then gradually decreased until 120 min (Fig. 2(b)). These results indicate that the increase in $|\mu|$ is most likely caused by the presence of MAc-rich polymers on the surface of the core microgels, while the decrease is caused by the presence of NIPAm-rich polymers on the surface of the developing microgels, resulting in the charged groups being localized at the interior of the first shell layer. It is worth noting here that $|\mu|$ did not approach 0 m^2 $(V\ s)^{-1}$, not even after more than 7 h of polymerization, without the addition of extra shell monomer (Fig. S2, ESI), indicating that a small amount of MAc is located on the

outer surface of the microgels. In contrast, the gradual increase in $|\mu|$ after the second addition of shell monomer (NIPAm, FAc, and BIS) suggests that FAc-rich polymers are present on the surface of the C-S(2) microgels (Fig. 2(b)).

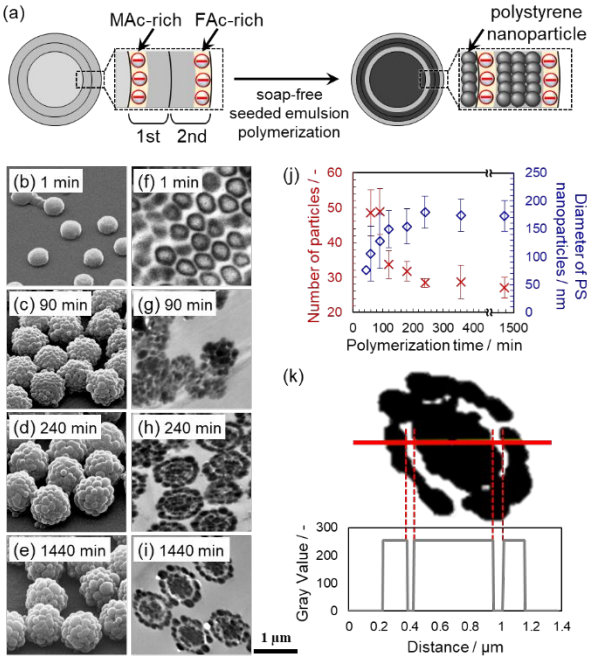

Fig. 3 (a) Schematic illustration of polystyrene-composite C-S(2) microgels obtained *via* soap-free seeded emulsion polymerization. Evolution of the composite microgels monitored *via* (b)–(e) FE-SEM images and (f)–(i) TEM images of ultra-thin cross-sections. Polystyrene was stained black using RuO_4. (j) Time dependence of the diameter (blue) and the number (red) of polystyrene nanoparticles on the composite microgel surface. (k) Analysis of the MAc-rich polymer electrolyte layer based on the TEM image, which was taken at 1440 min as shown in (i).

Next, to investigate the charge distribution of the C-S(2) microgels, composite microgels were synthesized *via* seeded emulsion polymerization of styrene in the presence of the microgels (Fig. 3(a)). Here, we assumed that polystyrene nanoparticles were polymerized and attached in the pNIPAm-rich regions in order to avoid the charged (carboxyl) groups of MAc and FAc (Fig. 3(a)), considering that the hydrophobic styrene monomer recognizes the polar region inside the microgels at the molecular scale and thus prefers to polymerize and attach in the almost uncharged regions inside the microgels.[17,19] The representative FE-SEM images of the composite C-S(2) microgels show that polystyrene nanoparticles were gradually composited into the microgels as the polymerization proceeded (Fig. 3(b–e)(j) and Fig. S3, ESI). Ultra-thin cross-sections of the developing composite microgels were observed using TEM to examine the distribution of polystyrene nanoparticles in the inner structure of the microgels (Fig. 3(f–i)). The polystyrene nanoparticles were distributed near the surface of the microgels during the initial stage of polymerization (c.a. 1 min), before polystyrene could also be observed in the center part (Fig. 3(f–i)). During the later stage of the polymerization, a 63 ± 24 nm region in the shell in which polystyrene nanoparticles were not distributed was observed, which was attributed to the MAc-rich polyelectrolyte region near the surface of the core (Fig. 3(k)). Furthermore, the thickness of the MAc-rich polyelectrolyte layer was controlled by varying the amount of shell monomers used in the preparation (Fig. S4, ESI). Thus, similar to the conventional precipitation polymerization of pNIPAm-based microgels,[18,19,22] the spatial distribution of the charged comonomers can be effectively controlled in each shell layer by using the pronounced difference in the reactivity between NIPAm and MAc or FAc.

Finally, to clarify the expandability of the synthetic technique to the production of CS microgels with additional layers, we conducted a one-pot polymerization with more monomer additions. As shown in Fig. 4, CS microgels with five shell layers (i.e., C-S(5) microgels) were successfully obtained. The resultant CS microgels were uniform in size and the formation of secondary microgels was not observed (Fig. 4b). We used DLS to clarify the dynamics of the polymerization, which revealed that the D_h of the microgels increases gradually and reaches a constant value after each addition (i.e., D_h = 245 nm at 60 min → 407 nm at 120 min → 568 nm at 180 min) (Fig. 4(a)). However, in the case of the 3rd, 4th, and 5th additions, the D_h increased slowly over 1 h on account of the decreasing radical concentration in the flask with increasing polymerization time and shell monomer addition (Fig. 4(a)). Simultaneously, the observed periodic changes in $|\mu|$ suggest that each shell layer exhibits a charge distribution (Fig. 4(a)). The seeded emulsion polymerization of styrene in the presence of C-S(5) microgels clearly confirmed the formation of CS microgels with four polystyrene-free layers (Fig. 4(c)(d)).

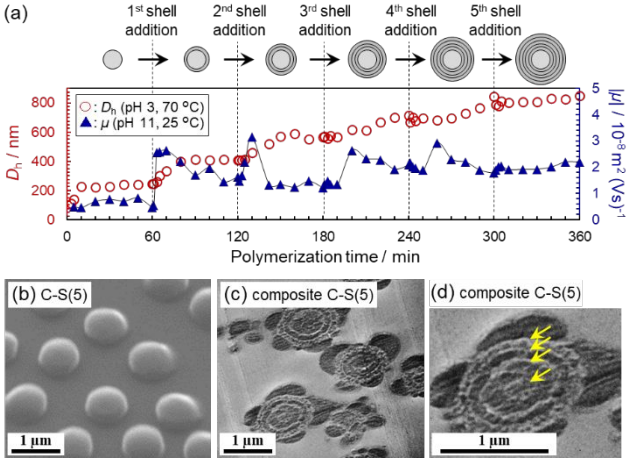

Fig. 4 (a) D_h and $|\mu|$ for C-S(5) microgels under different temperature/pH conditions at different polymerization times. (b) Representative FE-SEM image of C-S(5) microgels (D = 962 ± 37 nm, CV 3.9%, N = 200). (c,d) TEM images of the ultra-thin cross-sections of composite C-S(5) microgels.

At present, we think that these methodologies to produce CS microgels with multiple layers and their nanocomposites with rigid polymers can be developed further; for instance, the number of shell layers can most likely be increased by simply increasing the number of additions of shell monomers, and the chemical species of hydrogels are not necessarily limited to acrylamide derivatives, which will allow the construction of microgels suitable for biomedical applications, including drug-delivery systems, in which a more precisely controlled inner structure is required. Moreover, it has already been clarified that such composite microgels are useful for controlling the functions and properties of microgel-stabilized emulsions[23] and foams.[24] In addition, the assembly of CS microgels with internal complexity would be beneficial for the production of mechanically robust materials.[25] Therefore, this study represents an important first step toward creating advanced materials composed of functional CS microgels with multiple layers and their composites,

which will be useful in the fields of biomaterials and sustainable chemistry.

Conclusions

In this study, a new methodology to produce multi-layer core/shell (CS) microgels composed entirely of hydrogels was realized *via* a one-pot precipitation polymerization with the addition of shell monomers to the reaction flask. To clarify the structure of the complex CS microgels and their composites, a combination of structural characterization techniques including dynamic light scattering (DLS), electrophoretic light scattering (ELS), and microscopy was applied. A labelling method based on the seeded emulsion polymerization of styrene in the presence of such CS microgels allowed their internal structures to be clearly visualized, which revealed that the distribution of charged (carboxyl) groups can be controlled using the comonomer reactivity ratios (i.e., NIPAm with MAc or FAc) to occur on the inside or outside of each individual shell layer. Our findings thus provide new insights for applications where precisely structured microgels are crucial, including drug-delivery systems.

D.S. acknowledges a CREST Grant-in-Aid (JPMJCR21L2) from the Japan Science and Technology Agency (JST). H.M. acknowledges a Grant-in-Aid for Research Activity Start-up (20K22526) from Japan Society for the Promotion of Science (JSPS), a Grant-in-Aid (No. 731) from the Kose Cosmetology Research Foundation, and a Grant-in-Aid from the Foundation for Interaction in Science & Technology.

Conflicts of interest

There are no conflicts to declare.

Notes and references

1. (a) S. Nayak, L. A. Lyon, *Angew. Chem., Int. Ed.*, 2005, **44**, 7686–7708; (b) Y. Hoshino, K. Imamura, M. Yue, G. Inoue, Y. Miura, *J. Am. Chem. Soc.*, 2012, **134**, 18177–18180; (c) T. Kureha, Y. Nishizawa, D. Suzuki, *ACS Omega*, 2017, **2**, 7686–7694; (d) T. Kureha, D. Suzuki, *Langmuir*, 2018, **34**, 837–846; (e) S. Matsui, K. Hosho, H. Minato, T. Uchihashi, D. Suzuki, *Chem. Commun.,* 2019, **55**, 10064–10067.
2. (a) W. Richtering, *Langmuir*, 2012, **28**, 17218–17229; (b) M. Takizawa, Y. Sazuka, K. Horigome, Y. Sakurai, S. Matsui, H. Minato, T. Kureha, D. Suzuki, *Langmuir*, 2018, **34**, 4515–4525; (c) H. Minato, M. Murai, T. Watanabe, S. Matsui, M. Takizawa, T. Kureha, D. Suzuki, *Chem. Commun.*, 2018, **54**, 932−935; (d) M. Rey, M. A. Fernandez-Rodriguez, M. Karg, L. Isa, N. Vogel, *Acc. Chem. Res.*, 2020, **53**, 414–424; (e) A. Scotti, M. F. Schulte, C. G. Lopez, J. J. Crassous, S. Bochenek, W. Richtering, *Chem. Rev.*, 2022, **122**, 11675–11700.
3. (a) R. Pelton, *Adv. Colloid Interface Sci.*, 2000, **85**, 1– 33; (b) D. Suzuki, T. Sakai, R. Yoshida, *Angew. Chem., Int. Ed*., 2008, **47**, 917–920; (c) D. Suzuki, K. Horigome, T. Kureha, S. Matsui, T. Watanabe, *Polym. J*., 2017, **49**, 695–702; (d) M. Karg, A. Pich, T. Hellweg, T. Hoare, L. A. Lyon, J. J. Crassous, D. Suzuki, R. A. Gumerov, S. Schneider, I. I. Potemkin, W. Richtering, *Langmuir*, 2019, **35**, 6231–6255; (e) K. Inui, I. Saito, R. Yoshida, H. Minato, D. Suzuki, *ACS Appl. Polym. Mater.*, 2021, **3**, 3298–3306.
4. (a) T. Hellweg, C. D. Dewhurst, E. Brückner, K. Kratz, W. Eimer, *Colloid Polym. Sci.*, 2000, **278**, 972–978; (b) J. Mattsson, H. M. Wyss, A. Fernandez-Nieves, K. Miyazaki, Z. Hu, D. R. Reichman, D. A. Weitz, *Nature*, 2009, **462**, 83–86; (c) D. Suzuki, T. Yamagata, K. Horigome, K. Shibata, A. Tsuchida, T. Okubo, *Colloid Polym. Sci.*, 2012, **290**, 107–117; (d) S. Minami, D. Suzuki, K. Urayama, *Curr. Opin. Colloid Interface Sci.*, 2019, **43**, 113–124.
5. (a) G. R. Hendrickson, M. H. Smith, A. B. South, L. A. Lyon, *Adv. Funct. Mater*., 2010, **20**, 1697–1712; (b) J. Oberdisse, T. Hellweg, *Colloid Polym. Sci.*, 2020, **298**, 921–935.
6 (a) H. Ohshima, K. Makino, T. Kato, K. Fujimoto, T. Kondo, H. J. Kawaguchi, *Colloid Interface Sci.*, 1993, **159**, 512–514; (b) M. Ballauff, Y. Lu, *Polymer*, 2007, **48**, 1815–1823; (c) A. Rauh, T. Honold, M. Karg, *Colloid Polym. Sci.*, 2016, **294**, 37–47; (d) T. Kureha, Y. Nagase, D. Suzuki, *ACS Omega*, 2018, **3**, 6158–6165; (e) Y. Nishizawa, K. Honda, M. Karg, D. Suzuki, *Colloid Polym. Sci.*, 2022, **300**, 333–340; (f) H. Minato, Y. Sasaki, K. Honda, T. Watanabe, D. Suzuki, *Adv. Mater. Interfaces*, 2022, **9**, 2200879.
7. C. D. Jones, L. A. Lyon, *Macromolecules*, 2000, **33**, 8301–8306.
8. (a) D. Suzuki, J. G. McGrath, H. Kawaguchi, L. A. Lyon, *J. Phys. Chem. C*, 2007, **111**, 5667–5672; (b) X. Hu, Z. Tong, L. A. Lyon, *J. Am. Chem. Soc.*, 2010, **132**, 11470–11472; (c) J. Dubbert, K. Nothdurft, M. Karg, W. Richtering, *Macromol. Rapid Commun.,* 2015, **36**, 159–164; (d) A. J. Schmid, J. Dubbert, A. A. Rudov, J. S. Pedersen, P. Lindner, M. Karg, I. I. Potemkin, W. Richtering, *Sci. Rep.*, 2016, **6**, 22736.
9. (a) L. S. Zha, Y. Zhang, W. L. Yang, S. K. Fu, *Adv. Mater.*, 2002, **14**, 1090–1092; (b) S. Nayak, D. Gan, M. J. Serpe, L. A. Lyon, *Small,* 2005, **1**, 416–421.
10. (a) S. Wu, J. Dzubiella, J. Kaiser, M. Drechsler, X. Guo, M. Ballauff, Y. Lu, *Angew. Chem., Int. Ed.*, 2012, **51**, 2229–2233; (b) X. Hu, Z. Tong, L. A. Lyon, *Macromol. Rapid Commun.*, 2011, **32**, 1461–1466.
11. K. Honda, Y. Sazuka, K. Iizuka, S. Matsui, T. Uchihashi, T. Kureha, M. Shibayama, T. Watanabe, D. Suzuki, *Angew. Chem., Int. Ed.,* 2019, **58**, 7294–7298.
12. Y. Nishizawa, H. Minato, T. Inui, T. Uchihashi, D. Suzuki, *Langmuir*, 2021, **37**, 151–159.
13. C. D. Jones, L. A. Lyon, *Macromolecules*, 2003, **36**, 1988–1993.
14. (a) P. B. Zetterlund, Y. Kagawa, M. Okubo, *Chem. Rev.*, 2008, **108**, 3747–3794; (b) H. Yabu, *Bull. Chem. Soc. Japan.*, 2012, **85**, 265–274.
15. (a) I. Berndt, J. S. Pedersen, W. Richtering, *J. Am. Chem. Soc.*, 2005, **127**, 9372–9373; (b) I. Berndt, C. Popescu, F.-J. Wortmann, W. Richtering, *Angew. Chem., Int. Ed*., 2006, **45**, 1081–1085.
16. C. D. Jones, J. D. McGrath, L. A. Lyon, *J. Phys. Chem. B*, 2004, **108**, 12652–12657.
17. T. Watanabe, Y. Nishizawa, H. Minato, C. Song, K. Murata, D. Suzuki, *Angew. Chem., Int. Ed.,* 2020, **59**, 8849–8853.
18. T. Hoare, R. Pelton, *Curr. Opin. Colloid Interface Sci.*, 2008, **13**, 413–428.
19. T. Watanabe, C. Kobayashi, C. Song, K. Murata, T. Kureha, D. Suzuki, *Langmuir*, 2016, **32**, 12760–12773.
20. M. Heskins, J. E. Guillet, *J. Macromol. Sci., Part A: Pure Appl. Chem.*, 1968, **2**, 1441–1455.
21. A. Scotti, U. Gasser, E. S. Herman, M. Pelaez-Fernandez, J. Han, A. Menzel, L. A. Lyon, A. Fernández-Nieves, *Proc. Natl. Acad. Sci. U.S.A.*, 2016, **113**, 5576–5581.
22. Y. Nishizawa, T. Inui, R. Namioka, T. Uchihashi, T. Watanabe, D. Suzuki, *Langmuir*, 2022, **38**, 16084–16093.
23. T. Watanabe, M. Takizawa, H. Jiang, T. Ngai, D. Suzuki, *Chem. Commun.*, 2019, **55**, 5990–5993.
24. Y. Nishizawa, T. Watanabe, T. Noguchi, M. Takizawa, C. Song, K. Murata, H. Minato, D. Suzuki, *Chem. Commun.*, 2022, **58**, 12927–12930.
25. (a) T. Watanabe, H. Minato, Y. Sasaki, S. Hiroshige, H. Suzuki, N. Matsuki, K. Sano, T. Wakiya, Y. Nishizawa, T. Uchihashi, T. Kureha, M. Shibayama, T. Takata, D. Suzuki, *Green Chem*., 2023, **25**, 3418–3424; (b) Y. Sasaki, Y. Nishizawa, T. Watanabe, T. Kureha, K. Uenishi, K. Nakazono, T. Takata, D. Suzuki, *Langmuir*, 2023, **26**, 9262–9272.

